



HAL
open science

Effect of an excess of surfactant on thermophoresis, mass diffusion and viscosity in an oily surfactant-stabilized ferrofluid

Viesturs Sints, Mitradeep Sarkar, Jesse Riedl, Gilles Demouchy, Emmanuelle Dubois, Régine Perzynski, Dmitry Zablotsky, Gunars Kronkalns, Elmars Blums

► To cite this version:

Viesturs Sints, Mitradeep Sarkar, Jesse Riedl, Gilles Demouchy, Emmanuelle Dubois, et al.. Effect of an excess of surfactant on thermophoresis, mass diffusion and viscosity in an oily surfactant-stabilized ferrofluid. *European Physical Journal E: Soft matter and biological physics*, 2022, 45 (5), pp.43. 10.1140/epje/s10189-022-00200-7 . hal-03872864

HAL Id: hal-03872864

<https://hal.science/hal-03872864>

Submitted on 25 Nov 2022

HAL is a multi-disciplinary open access archive for the deposit and dissemination of scientific research documents, whether they are published or not. The documents may come from teaching and research institutions in France or abroad, or from public or private research centers.

L'archive ouverte pluridisciplinaire **HAL**, est destinée au dépôt et à la diffusion de documents scientifiques de niveau recherche, publiés ou non, émanant des établissements d'enseignement et de recherche français ou étrangers, des laboratoires publics ou privés.



Distributed under a Creative Commons Attribution - NonCommercial - NoDerivatives 4.0 International License

Effect of an excess of surfactant on thermophoresis, mass diffusion and viscosity in an oily surfactant-stabilized ferrofluid

Viesturs Sints^{a,1}, Mitradeep Sarkar², Jesse Riedl², Gilles Demouchy^{2,3},
Emmanuelle Dubois², Régine Perzynski², Dmitry Zablotsky¹, Gunars
Kronkalns¹, Elmars Blums¹

¹ Institute of Physics, University of Latvia, Miera 32, Salaspils LV-2169, Latvia

²Sorbonne Université - CNRS - Lab. PHysico-chimie des Electrolytes et Nanosystèmes Interfaciaux (PHENIX), case 51- 4 place Jussieu, F-75005 Paris, France

³Dpt de Physique - Univ. Cergy-Pontoise, 33 Bd du port 95011 Cergy-Pontoise, France

Received: date / Accepted: date

Abstract The effect of an excess of surfactant on the thermophoresis of a sterically stabilized ferrofluid is investigated experimentally by Forced Rayleigh scattering (FRS). The experiments are performed with a stable magnetic fluid sample to which controlled amounts of surfactant are added. A decrease in the thermally induced transport of magnetic nanoparticles is observed while increasing the temperature T . The positive Soret coefficient S_T decreases by adding 2 vol% of surfactant at room temperature. As shown by FRS relaxation, this decreasing is mainly associated to a reduction of the interaction between the carrier fluid and individual nanoparticles. No significant effect of extra surfactant on the sign of S_T is observed at higher T 's (up to $\sim 85^\circ\text{C}$). Dynamic Light Scattering (DLS) at room temperature reveals the presence of a small amount of clusters/ aggregates in the samples, which are hardly detectable by FRS relaxation. The presence of these small clusters/ aggregates is confirmed by a rheological probing of the fluid properties. Whatever T , a small amount of added surfactant first causes a decrease of the ferrofluid viscosity, associated to a 10% decreasing of the flow activation energy. Further on, viscosity and activation energy, both recover at higher excess surfactant concentrations. These results are analyzed in terms of saturation of the surfactant layer, concentration of free surfactant chains and heat of transport of the nanoparticles.

1 Introduction

We investigate experimentally the effects of an excess of surfactant on several physical properties of oily ferrofluids, particularly those connected with temperature and thermally induced particle transfer. Ferrofluids based on magnetite nanoparticles (NPs) dispersed in tetradecane as carrier fluid with oleic acid (OA) as surfactant are probed here. OA is progressively added to the ferrofluid after the synthesis process, during which NPs were OA-coated to ensure the ferrofluid colloidal stability.

The interest in ferrofluid behavior when subjected to a temperature gradient is generally driven by a variety of applications for this class of colloids in relation with heat transfers. Historically, the first application has been loudspeaker cooling, while novel examples include solar collectors [1], electrochemical thermal en-

ergy harvesters [2] and cooling of electronic devices [3]. Exploring how the response of a surfactant stabilized colloid, to a gradient of temperature depends on its composition can improve the ability to tune such colloids to the specific purpose [4–6].

To this end, several studies have been performed in polar media (i) in ferrofluids based on charged nanoparticles by varying ionic strength or the nature of the ionic moieties, see for example Refs. [7–11] and (ii) in non-magnetic dispersions of polystyrene beads by addition of ionic surfactant [4, 12, 13]. To our knowledge, such systematic studies about colloidal dispersions stabilized by an oily surfactant in oily media (or even in organic solvents) are however rather scarce. The study by Ning *et al.* [14] on dispersions of nanosilica grafted with octadecyl groups in toluene can be quoted in this regards.

Previous research has shown that oily ferrofluids in a porous environment can present a decrease in thermally induced particle transport [15] for a wide range

^ae-mail: viesturs.sints@lu.lv

of such colloidal dispersions [16,17]. It has also been shown that surfactant addition further decreases Soret coefficient in a porous medium and that, at a sufficient concentration of excess surfactant, the particle transfer direction in a temperature gradient can be inverted [17]. In that matter, uncertainty remains regarding the relative importance of colloidal processes and the porous medium itself in the aforementioned findings. The effect of a double-layer of surfactant on modifying the value and the sign of the Soret coefficient of polystyrene nanobeads in aqueous dispersions has been shown both by O. Syshchyk *et al.* [13] and by Q. Jiang *et al.* [4]. Studies of thermophoresis in a porous medium have reported both lack of deviation from free fluid values for Soret coefficient in binary mixtures [18] and reduction of Soret coefficient in pores due to confinement effects in alkali halide aqueous solutions [19]. However, a reference regarding oily colloids, in question here, is lacking. The work presented here can help gaining further insight into the effects of free surfactant concentration in an oily colloid. It will also validate if the aforementioned phenomena concerning such oily ferrofluids are present outside of a porous environment or not.

Research about such physical phenomena presents a challenge, as there is no universally accepted theoretical interpretation for thermophoresis of such colloidal dispersions [20,21]. A variety of theoretical models [22–25] exist to describe the mechanisms for particle thermophoresis in such colloidal liquids, a dominant effect coming here from the NP/ complex fluid interaction [26]. In the case of electrostatically charged nanoparticles dispersed in a polar solvent a link to Seebeck effect is put forward [9,10,27]. It is however not the case here. The model proposed by Morozov [25] describes the colloidal particle thermophoresis as driven by interaction between the particles and smaller species, like surfactant molecules - specifically for surfactant stabilized colloids. This approach would predict particle migration toward lower temperatures driven by the benefit of a colloidal particle placed in a temperature gradient to be able to adsorb more surfactant molecules in the colder side than in the hotter one. Parola and Piazza [28] arrived to an expression for the Soret coefficient that involves a relation between surface tension and temperature. Works by Iacopini and Piazza [29] and Iacopini *et al.* [30] describe particle thermophoresis in aqueous media with an emphasis on its temperature dependence, including a change of particle transfer direction at a certain temperature. Because of this sign inversion of the Soret coefficient, this phenomenological expression has been adapted in Ref. [17] to be correlated with the experimental observations of an oily ferrofluid in a porous environment.

From the rheological point of view, on the nanoscale and on the macroscopic scale, well dispersed ferrofluids are dilute to moderately concentrated suspensions [31] and ferrofluid viscosity decreases with temperature, driven by the viscosity of the carrier fluid [32], see also for example the dispersions in glycerol of Abareshi *et al.* [33] and those in transformer oil of Tothova *et al.* [34].

We therefore investigate here thermophoresis of NPs coated with oleic acid in a free-fluid ferrofluid based on tetradecane, with an excess of added surfactant with respect to synthesis conditions. To complement the thermophoretic investigation of the system, the mass diffusion coefficient of the NPs is here probed by two different techniques with and without the addition of 2 vol% of surfactant. Dynamic light scattering probes the thermal fluctuations of NP's concentration at 20°C in unperturbed dispersions, while relaxation of forced Rayleigh scattering probes the relaxation of a concentration modulation at a well defined scattering vector [35], from room temperature up to $\sim 85^\circ\text{C}$. Rheological measurements of the ferrofluid dispersions complete here the presented work, in a large range of temperatures and added surfactant concentrations. They are compared to the tetradecane viscosity measurements from [17] and discussed in the framework of all the presented results.

2 Theoretical framework

2.1 Soret coefficient

Thermophoretic transfer of a nanoparticle in a solvent is characterized by the Soret coefficient S_T . It is defined as the relation between thermodiffusion and mass diffusion coefficients.

$$S_T = \frac{D_T}{D_m} \quad (1)$$

In stationary conditions, as in the FRS experimental device used in Sect. 4.1 and with uncharged colloidal nanoparticles, the Soret coefficient expresses at the first order¹ as [9,27]:

$$S_T \sim \chi \frac{\hat{S}_{\text{NP}}}{kT}. \quad (2)$$

The compressibility χ of the NP's system characterizes the interparticle interaction. It is related to the derivative of the osmotic pressure Π with respect to the number of NPs per unit volume n_{NP} through $\chi = kT / \frac{\partial \Pi}{\partial n_{\text{NP}}}$.

¹We neglect here the term $\frac{1}{n_{\text{NP}} kT} \frac{\partial \Pi}{\partial T}$ in front of $\frac{\hat{S}_{\text{NP}}}{kT}$, as it is here always smaller than 9.10^{-3} K^{-1} .

The NP Eastman entropy of transfer \hat{S}_{NP} characterizes the affinity of the NPs with the fluid carrier. It is a thermodynamic quantity [36] defined as the ratio of the enthalpy (heat) of transport Q^* of the NPs divided by T [37], kT being the thermal energy. Q^* quantifies the thermophobicity of the system [38].

Note that here, due to the low volume fraction of oleic acid, we assimilate the ternary system (OA-coated NPs, tetradecane, free OA) to a binary system (OA-coated NPs, fluid carrier)². In this approximation, the NP Eastman entropy of transfer \hat{S}_{NP} may contain a contribution from diffusiophoresis of free OA chains as in the aqueous ferrofluids of [8] with added organic salts.

In aqueous media Iacopini and Piazza [29] have proposed an empirical model which works in many situations associated with H-bond interactions:

$$S_{\text{T}}(T) = S_{\text{T}}^{\infty} \left[1 - \exp\left(\frac{T^* - T}{T_0}\right) \right] \quad (3)$$

In this expression, T^* is the temperature at which $S_{\text{T}} = 0$ and T_0 characterizes the strength of temperature effects on Soret coefficient. The authors refer to S_{T}^{∞} as a high temperature limit for the Soret coefficient. However in the work shown in [17], the ferrofluid displayed a low temperature "plateau" of Soret coefficient, followed by a decrease as temperature increases. Therefore, without surprise, this expression cannot work as it is, in our oily system, as the notion of high temperature limit is not suitable in our case. A coefficient $S_{\text{T},1}$ is introduced to be used instead, to acknowledge this difference. A sign change of coefficient T^* and temperature is motivated by experimental observations of S_{T} reducing with temperature increase in our colloid. After this, we obtain the empirical equation used here to describe $S_{\text{T}}(T)$:

$$S_{\text{T}}(T) = S_{\text{T},1} \left[1 - \exp\left(\frac{T - T^*}{T_0}\right) \right] \quad (4)$$

Let us note that other expressions, such as for example that of G. Wittko and W. Kohler [39] proposed for solvent mixtures, could be used successfully to take in account both the concentration and the temperature dependence of Soret coefficient for ionic species added to water [40]. However this expression is also empirical.

2.2 Diffusion coefficient

The mass diffusion coefficient D_{m} of the NPs is related to the thermal energy kT , to the friction ζ experienced

²Fluid carrier = tetradecane + dissolved free OA chains

by the NPs and to the compressibility χ of the NPs system in the colloidal dispersion through the generalized Stokes equation [41, 42]:

$$D_{\text{m}} = \frac{1}{\zeta} \frac{kT}{\chi} \quad (5)$$

Assimilating here the NPs to Hard Spheres of volume fraction $\Phi \sim 5\%$ as in [17], the Carnahan-Starling model [9, 43] leads to $\chi \sim 0.67$ ³. Moreover as according to [44], the friction can be written for Hard Spheres as $\zeta \sim \zeta_0/(1 - 6.55\Phi)$ at low Φ 's, we thus obtain $\zeta \sim 1.49\zeta_0$ at $\Phi \sim 5\%$ and here $\zeta\chi \sim 0.99\zeta_0$. Then the mass diffusion coefficient D_{m} of the NPs writes at the first order as:

$$D_{\text{m}} \sim \frac{kT}{3\pi\eta_0 d_{\text{h}}}, \quad (6)$$

where η_0 is the pure solvent viscosity and d_{h} the NP's hydrodynamic diameter.

2.3 Viscosity

For colloids with an effective hydrodynamic volume fraction Φ_{h} up to 10%, the relative dynamic viscosity $\eta_{\text{r}} = \eta/\eta_0$ should follow the Batchelor formula [31, 45]:

$$\eta_{\text{r}} = \eta/\eta_0 = (1 + 2.5\Phi_{\text{h}} + 6.2\Phi_{\text{h}}^2) \quad (7)$$

This expression is valid up $\eta_{\text{r}} \sim 1.3$. For $\eta_{\text{r}} \geq 1.3$, the expression from C.L. Berli and D. Quemada [46] in [45] is more appropriate:

$$\eta_{\text{r}} = \frac{1}{1 - (\Phi_{\text{h}}/0.63)^2} \quad (8)$$

To describe temperature dependence of viscosity, we use the Arrhenius model:

$$\eta = \eta_{\infty} \exp\left(\frac{E_{\text{a}}}{kT}\right) \quad (9)$$

Here, η is the dynamic viscosity, η_{∞} is the viscosity at "infinite temperature" and E_{a} denotes the activation energy of the fluid.

³We suppose here that χ is associated to the entropic effect of excluded volume of the hard spheres, leading to an effective interparticle interaction with a second virial coefficient $A_2 = 4$. We implicitly suppose that the hard sphere volume is here, at the first order, independent of the concentration of added surfactant. This point is discussed in Sects. 6 and 2 of E.S.I., where the value of $\zeta\chi$ is also discussed.

3 Ferrofluid used in experiments

The colloid used in thermophoresis experiments is a surfactant stabilized ferrofluid. Magnetic single-domain nanoparticles are dispersed in a carrier fluid and stabilized with an adsorbed layer of molecules of surfactant around the particles to prevent the NP's agglomeration and to ensure a strong interaction between the NP's and the dispersion medium. The ferrofluid is prepared in Institute of Physics, University of Latvia, by chemical coprecipitation, following the procedure described in Ref. [47]. The preparation procedures involve a centrifugation of the colloid at 7000 g, a separation in high magnetic field gradients (HGMS) and a flocculation process employed to remove from the initial colloidal sample the excess of surfactant (i.e. the part not chemically bounded with nanoparticles). It is comparable to what is done for the samples of the SANS study of [48]. The particle material is Fe_3O_4 , the carrier fluid is tetradecane and the surfactant coating the NPs is oleic acid (OA). The mean particle diameter, as determined by vibrating sample magnetometry using Lake Shore Cryotronics Co., model 7404 VSM vibrating sample magnetometer [49], is $d_{\text{magn}} = 9.6$ nm and the volume fraction of magnetic material is $\Phi = 4.75\%$. The tetradecane used for the preparation of the ferrofluid and in the present experiments is provided by Sigma-Aldrich, as is the oleic acid. The viscosity of tetradecane at 20°C is $2.29 \cdot 10^{-3}$ Pa.s, according to [50]. The oleic acid ($\text{C}_{18}\text{H}_{34}\text{O}_2$) is a non-saturated mono-carboxylic (fatty) acid, fully soluble in tetradecane. It presents a C18-tail with a double bond kink in the middle. Its polar head adsorbs on the surface of the NPs by chemisorption [51], while hydrophobic tails dissolve in tetradecane, forming a monolayer of surfactant chains at the NP surface [52].

Due to the preparation procedures of the ferrofluid, a very large part of the oleic acid present in the initial ferrofluid is bound to the nanoparticles⁴, in a way comparable to what is observed in the Small Angle Neutron Scattering of [48] in decahydronaphtalene. In this latter work, the thickness of the oleic acid layer on the surface of the nanoparticles is determined to be 1.40 ± 0.07 nm⁵, to be compared to the theoretical value 2.3 nm deduced from Tanford formula [54].

Another study of interest to fix order of magnitudes is that of E. Dubois et al [55] studying maghemite NPs coated with oleic acid and dispersed in cyclohexane, which is focusing on the adsorption isotherm of OA at

⁴Note that due to the adsorption process, the concentration of free OA at equilibrium in solution, which is small, is however not strictly zero.

⁵A compatible value 1.38-1.43 for the OA-layer is found in the rheological study of ferrofluids in transformer oil [53].

room temperature. It leads to a saturation value of 3.6 molecules of OA per nm^2 , which can be considered as close to the one for the present system. Moreover a determination by SANS of the pair interparticle interaction parameter $A_2 = 4.4 \pm 0.6$ (compatible with the hard sphere value of 4) is also obtained in this work for NPs with a saturated coating. A former thermodiffusion study on this system has pointed out at room temperature a thermophobic behavior for these NPs coated with oleic acid and dispersed in cyclohexane [26].

For the experiments with an excess of surfactant in the colloid, oleic acid is added at a concentration c varying from 0 up to 2.5 vol%. As tetradecane is non-polar and oleic acid fully soluble in tetradecane, micelle formation is energetically unfavorable in the anhydrous medium [56,57]. Anyway, DLS tests have been performed in a solution of oleic acid in tetradecane at 2.5 vol% and no oleic acid structures could be detected. Such an experimental conclusion has been also obtained in two SANS studies of OA-coated magnetic NPs up to 25 vol% of added OA in deuterated non-polar solvents, namely [58] in benzene and [59] in decaline. In these two studies, in presence of added surfactant, the thickness of the oleic acid layer on the surface of the nanoparticles is respectively determined to be 1.40 (resp.1.43) ± 0.07 nm.

Note that the characteristic concentration value c for surfactant corresponds to the volumic fraction of surfactant added with respect to the initial sample issued from the synthesis process.

4 Experimental methods

4.1 Forced Rayleigh scattering

In the Forced Rayleigh Scattering (FRS) setup, fully described in [11], a 1D sinusoidal grid is imaged inside the volume of the ferrofluid, inserted in a thin optical cell of thickness 100 μm . The cell is placed in a thermo-regulated sample holder allowing to work here between room temperature and $T = 85^\circ\text{C}$. The colloidal particles of the ferrofluid absorb the incident light (a high power lamp, up to 500W- Hg Arc Lamp-240 Spectra Physics, is used as the illuminating source) and thus cause a periodic spatial-modulation of temperature (ΔT) in the sample with a modulation pitch Λ varying between 80 and 160 μm . These temperature gradients yield movements of the particles according to the Soret-Ludwig effect and this subsequently results in periodic spatial-modulation of volume fraction ($\Delta\Phi$) in the sample. These modulations of temperature and volume fraction can be considered as thin 1D-gratings. The corresponding refractive index modulations consist

of the contributions of both ΔT and $\Delta\Phi$. We can assume that the total refractive index modulation $\Delta n_{T\Phi}$ is a linear sum of the two contributions, namely the change in refractive index owing to the temperature gradient (Δn_T) and that owing to the concentration gradient (Δn_Φ). Thus it can be written as

$$\Delta n_{T\Phi} = \Delta n_T \pm \Delta n_\Phi \quad (10)$$

It should be noted that for positive Soret coefficients (when particles move to regions with lower temperatures) the temperature and volume fraction modulations are in antiphase while for negative Soret coefficients (particles move to higher temperatures) they are in phase. The variation of refractive index with temperature ($\partial n/\partial T$) is generally negative while its variation with the concentration ($\partial n/\partial\Phi$) is positive. So contributions of the temperature modulations and those of concentration to the total refractive index are additive for positive Soret coefficients while for negative Soret coefficients they oppose each other. The sign \pm in Eq.10 reflects these two situations.

These two gratings are studied by diffraction of a non-absorbing laser beam. The refractive index modulation of a thin sinusoidal volume grating with thickness d can be evaluated from the first order diffracted intensity (I_d) by the relation (given here at the first order)[60–62]

$$\Delta n \sim \frac{\lambda \cos(\theta)}{\pi d \sqrt{I_0}} \sqrt{I_d} \quad (11)$$

θ being the incidence angle (here, $\theta = 38^\circ$). To separate the influence of the concentration and temperature on the total refractive index modulation, a chopper is used to cut off the illumination and thus temporally modulate the heat source at the rate of 8 Hz. Here we assume that the thermal relaxation of the system is a rapid process (of the order of a few ms for grid periods of tens of μm) while the relaxation of the concentration gradient is rather slow (here of the order of several seconds). So when the heat source is cut off by the chopper (for about 63 ms per cycle), the intensity diffracted (I_Φ) and the corresponding (Δn_Φ) evaluated by Eq. 11 does not have any contribution from the temperature modulation of the grating. It is purely due to the concentration modulation ($\Delta\Phi$). This latter is not influenced by the chopper. So the temperature and volume fraction index modulations created in the ferrofluid at steady state can be evaluated from the values of the intensity diffracted during the chopper off cycle (I_Φ) and chopper on cycle ($I_{T\Phi}$) as

$$|\Delta\Phi| = \frac{|\Delta n_\Phi|}{(\partial n/\partial\Phi)_{c,T}} = \frac{\lambda \cos(\theta)}{\pi d \sqrt{I_0}} \sqrt{I_\Phi} \quad (12)$$

$$\Delta T = \left| \frac{\Delta n_T}{(\partial n/\partial T)_{c,\Phi}} \right| = \frac{\lambda \cos(\theta)}{\pi d \sqrt{I_0}} (\pm \sqrt{I_{T\Phi}} \mp \sqrt{I_\Phi}) \quad (13)$$

under the atmospheric pressure. In these expression, neglecting the contribution from free OA, the coefficient $(\partial n/\partial T)_{c,\Phi}$ is taken to be that of the carrier fluid, here tetradecane, so that $(\partial n/\partial T)_{c,\Phi} = -4.16 \cdot 10^{-4} \text{ K}^{-1}$ [63]. Coefficient $(\partial n/\partial\Phi)_{c,T}$ is taken from Maxwell Garnett approximation [64] which here equals 0.95.

At steady state the Soret coefficient can be evaluated as:

$$\Phi_0 S_T = - \frac{\Delta\Phi_{St}}{\langle \Delta T \rangle} \quad (14)$$

$\langle \Delta T \rangle$ being the mean temperature modulation and $\Delta\Phi_{St}$ the nanoparticle volume fraction modulation, at steady state. The mean temperature modulation is related to the maximum value of temperature modulation ΔT_m by a factor 1/2 as the duty cycle of the chopper during the experiment at steady state is 50%, so that $\langle \Delta T \rangle = \Delta T_m/2$.

In the present work, in a similar way as in the experiments of [11], it is checked that the obtained $\Delta\Phi$ is proportional to the obtained $\langle \Delta T \rangle$ by varying the power of the lamp up to 300 W and the modulation pitch in the range 92 to 156 μm . They vary in the range $\Delta\Phi \leq 0.2\%$ and $\langle \Delta T \rangle \leq 0.2 \text{ K}$. For the same $\langle \Delta T \rangle$, a larger $\Delta\Phi$ is obtained with the sample at 0 vol% of added OA with respect to the sample at 2 vol% of added OA.

4.2 Relaxation of forced Rayleigh scattering (FRS) and Dynamic light scattering (DLS)

The translational diffusion coefficient of the nanoparticles is measured here by two different techniques, forced Rayleigh scattering which analyses the relaxation of the spatial modulation of concentration, former induced by Soret effect at a well defined wave vector and Dynamic light scattering which analyses the fluctuations of NP's concentration, without any spatial distortion of the NP's organization [35].

In the forced Rayleigh scattering experiment, when the heat source is switched off after the Soret coefficient measurement, $\Delta T = 0$ and the relaxation of the

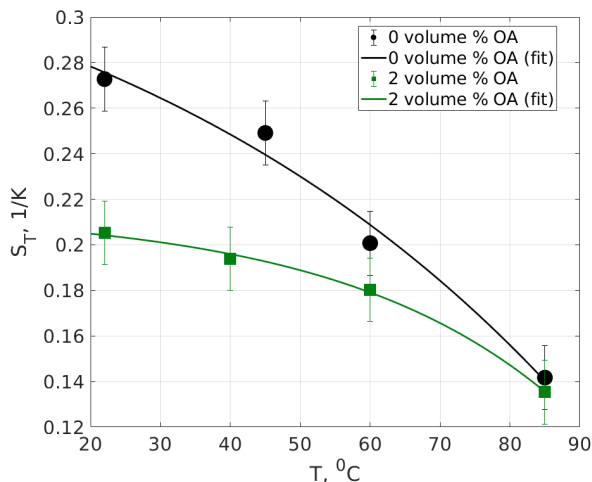


Fig. 1 Soret coefficient as a function of temperature, measured by FRS, along with its fitting by Eq. 4.

volume fraction modulation $\Delta\Phi$ undergoes a transient decay. If the relaxation is monoexponential, the diffusion coefficient D_m is deduced from the relaxation time $\tau_{\text{FRS}} = 1/q^2 D_m$ of the square root of the diffracted intensity, with $q = 2\pi/\Lambda$ the grating vector.

Dynamic light scattering measurements are made with a Vasco DLS Particle analyzer from Cordouan Technologies at room temperature. This apparatus works at 656 nm in back scattering at 135° , corresponding here to a scattering vector $Q = 2.5 \cdot 10^7 \text{ m}^{-1}$. It is adapted for strongly absorbing colloidal dispersions and allows the determination of the mass diffusion coefficient D_m of the NPs [65]. The intensity auto-correlation function $G(t)$ measured by the Vasco DLS Particle Analyzer is transformed into the field auto-correlation function $G_1(t)$ using the expression $G_1(t) = [G(t)]^{1/2} - \text{offset}$.

4.3 Rheological measurements

The viscosity of the fluid samples is measured with an Anton Paar MCR 502 rheometer, using a cone-plate setup. The rheometer is equipped with a Peltier temperature control, which allows us to perform measurements at various temperatures. Measurements are done in a continuous rotational mode.

5 Experimental results

5.1 Thermophoresis

Soret coefficients S_T obtained by FRS measurements, at $c = 0 \text{ vol}\%$ (without added surfactant) and at $c = 2$

$\text{vol}\%$ of added surfactant, are given in Fig. 1. In both situations and whatever the temperature, the measured S_T is positive and the NP behavior is clearly thermophobic. The Soret coefficient exhibits a significant decrease at $c = 2 \text{ vol}\%$ with respect to its value in the initial ferrofluid. This can be due to the interparticle interaction (χ variation in Eq. 2) or by the NP/complex fluid interaction (\hat{S}_{NP} variation in Eq.2). Both can be altered by the surfactant in excess in the carrier fluid and by surfactant adsorption on NPs, larger than the amount present at the end of the ferrofluid synthesis. Using $\chi = 0.67$ whatever c as proposed in Section 2.2 (see Sect. 6 for a critical analysis of this hypothesis), \hat{S}_{NP}/kT thus decreases at room temperature from $+0.4 \text{ K}^{-1}$ for $c = 0 \text{ vol}\%$ down to $+0.3 \text{ K}^{-1}$ for $c = 2 \text{ vol}\%$. These values are of the same order of magnitude as those observed at room temperature for example in [11] for charged NPs dispersed in DMSO-water mixtures at intermediate molar fractions of water (0.2 and 0.8 mol%). A marked decrease of \hat{S}_{NP}/kT with the temperature increase is also observed here, at 85°C , \hat{S}_{NP}/kT is of the order of $+0.2 \text{ K}^{-1}$, irrespectively to OA added concentration. In literature, very few experimental colloidal systems present both $S_T > 0$ and $\partial S_T/\partial T < 0$, we can quote the work by Fiuza et al [66] on ferrofluids dispersed in an Ionic Liquid and the work by Sehnen et al [8] on aqueous ferrofluids with two different added salts. While S_T is frequently negative in aqueous ferrofluids, see for example [9], in this latter study, S_T is positive with $\partial S_T/\partial T < 0$ with added TBAOH salt. However with a slightly smaller TMAOH salt they obtain $\partial S_T/\partial T > 0$.

In principle, in the present system, the complex-fluid interaction parameter \hat{S}_{NP} can be both related to a redistribution of surfactant and to the presence of free surfactant chains remaining in solution. An analogy could be made with the retardation of droplet thermophoresis by surfactant as described in Ref. [67], corresponding to the hindrance of surfactant molecules redistributed around the particle by local saturation in the layer. Indeed, saturation of colloidal particle surface with surfactant molecules has been identified as the mechanism behind a reduction of Soret coefficient for polystyrene beads [13] in aqueous media. The other mechanism to be considered here is diffusiophoresis of the colloidal particles in concentration gradients of free OA chains in the solution induced by molecular thermodiffusion. Indeed, it is experimentally observed in [8] in aqueous ferrofluids with added organic salts, that the T - and c_{salt} -dependence of the NP's Soret coefficient S_T correlate with that of the added species. Here diffusiophoresis related to free OA chains has to be named among the possible contributing mechanisms to the ob-

Table 1 Parameters of the empirical model (Eq.4) fitted to Soret coefficient measurements

c , vol%	$S_{T,1}$, K^{-1}	T^* , $^{\circ}C$	T_0 , $^{\circ}C$
0.0	0.37	118.6	70.2
2.0	0.22	116.3	31.4

served phenomena. However, the lack of thermodiffusion measurements of free OA chains in tetradecane and of direct measurements of free OA concentration in the ferrofluid prohibits us from developing solid further conclusions, at this step.

The Soret coefficient decreases with temperature in an exponential way, which is similar to what is seen in Soret coefficient measurements for the same ferrofluid samples in a porous environment, as described in Ref.[17]. However, no change of sign can be observed between $22^{\circ}C$ and $85^{\circ}C$ - this is true for samples both with and without added surfactant. Note nevertheless that the here measured values of S_T are much larger than these of Ref. [17] in porous media. The Soret coefficient is here analyzed as a function of temperature in the framework of the empirical model given by Eq. 4. The results are shown in Table 1.

Figure 1 and Table 1 show that the addition of an excess of surfactant (up to 2 vol% of OA) significantly modifies the temperature-dependence of S_T . The empirical parameter T_0 , associated with effect of temperature on S_T , has decreased, indicating a lessened temperature dependence of the Soret coefficient. It should be noted that both of those tendencies are in contrast to those seen in a porous environment, where addition of surfactant steepen the temperature dependence of S_T . This indicates that the previously observed influence of excess surfactant is an effect of interaction with the porous environment and not properties inherent to the ferrofluid itself.

5.2 Diffusion coefficient

Relaxation of forced Rayleigh scattering (FRS)

By FRS relaxation, the time evolution of the intensity $I_{\Phi}(t)$, normalized at $t = 0$ and proportional to the modulation $\Delta\Phi$ is here observed to be close to an exponential function of time.

Some examples of these results obtained at room temperature are displayed in Fig. 2-Bottom. This figure compares mono-exponential fits with respect to bi-exponential fits together with their residuals) in two examples at $T = 22^{\circ}C$ for 0 vol% (resp. 2 vol%) of added OA with two different spatial periods (see figure caption). For 0 vol% of added OA (resp.2 vol%) the

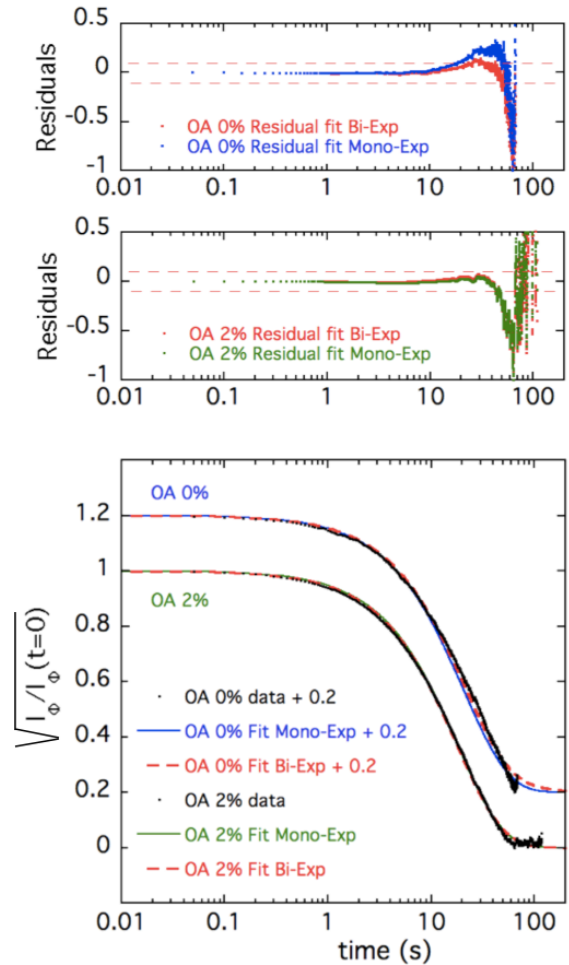


Fig. 2 Bottom: Two examples of time relaxation of the square-root of intensity $I_{\Phi}(t) \propto \Delta\Phi(t)$ normalized by $I_{\Phi}(t=0)$ at $T = 22^{\circ}C$ for 0 vol% (resp. 2 vol%) of added OA with a grid of spatial period $\Lambda = 92.5 \mu m$ (resp. $110 \mu m$) - For clarity OA 0 vol% is shifted vertically by +0.2; FRS data are black dots, full lines correspond to adjustments of the measurements by a single exponential relaxation; Dashed lines correspond to adjustments by a bi-exponential relaxation (see text for details). Top (resp. Middle): Residual fits at added OA 0 vol% (resp. 2 vol%) as defined as $(\sqrt{I_{\Phi}^{Exp}} - \sqrt{I_{\Phi}^{Fit}})/\sqrt{I_{\Phi}^{Fit}}$ as a function of time t for the mono-exponential and bi-exponential adjustments; Red dashed lines corresponds to $(\sqrt{I_{\Phi}^{Exp}} - \sqrt{I_{\Phi}^{Fit}})/\sqrt{I_{\Phi}^{Fit}} = \pm 10\%$.

mono-exponential fits leads to $D_m = 1.05 \cdot 10^{-11} m^2/s$ and $d_h = 18.0 nm$ (resp. to $D_m = 1.67 \cdot 10^{-11} m^2/s$ and $d_h = 11.2 nm$). Tentative bi-exponential fits are also presented in Fig. 2-Bottom. If an improvement is obtained at 0 vol% of added OA, by the addition of 5% in diffracted intensity, of NPs with $d_h = 87.0 nm$, the improvement given by the tentative adjustment at 2 vol% of added OA with 90% of $d_h = 10.4 nm$ and 10%

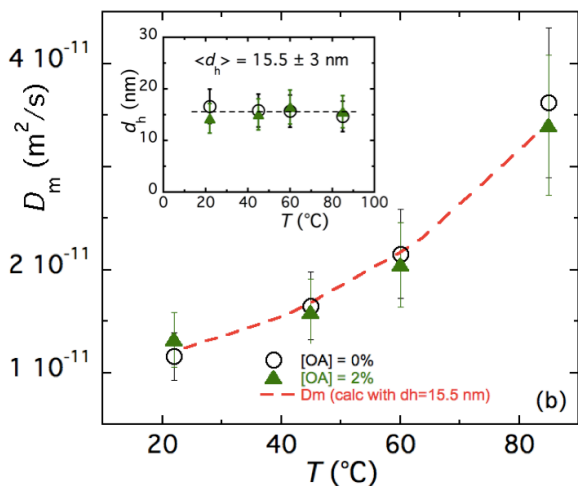


Fig. 3 Mass diffusion coefficient D_m deduced from a mono-exponential fit of the FRS relaxation (averaging at a given T over 3 to 6 measurements with grids of different Λ 's and several power of the heating beam) as a function of T for 0 vol% and 2 vol% of OA - Inset : Corresponding hydrodynamic diameter d_h as a function of T for 0 vol% and 2 vol% of OA.; The dashed line of the inset corresponds to the mean d_h value; The dashed line of the main figure corresponds to $D_m(T)$ obtained with Eq. 6 using the viscosity of tetradecane and $d_h = 15.5 \pm 3$ nm.

of $d_h = 18.4$ nm is not really convincing⁶. So, for sake of simplicity we further analyze FRS relaxation with a mono-exponential fit, keeping in memory, that some extra NPs' agglomerates are present at 0 vol% of added OA close to room temperature.

After averaging over 6 measurements (as those of Fig. 2, at the same T , with several grids of different Λ 's and several power of the heating beam) adjusted with a mono-exponential fit, the mean diffusion coefficient D_m and the mean NP's hydrodynamic diameter d_h are obtained using Eq. 6 with the known viscosity of pure solvent. They are given at room temperature in Table 2 and Fig. 3 shows the evolution of D_m and d_h as a function of T .

By FRS probing, we can see that the addition of an excess of surfactant does not have a significant impact on the mass diffusion coefficient deduced from the monoexponential adjustment. D_m increases with temperature, as one would expect due to decreasing of η with T . The associated values of the hydrodynamic diameter d_h , which are presented as a function of T for the two concentrations of added OA in the inset of Fig. 3 for the two samples at 0 vol% of OA and 2 vol% of OA show neither a significant evolution with T nor by adding an excess of surfactant, with a mean value $d_h = 15.5 \pm 3$ nm.

⁶The bi-exponential fit is as well not really convincing at $T = 85^\circ\text{C}$ for both 0 vol% and 2 vol% of added OA

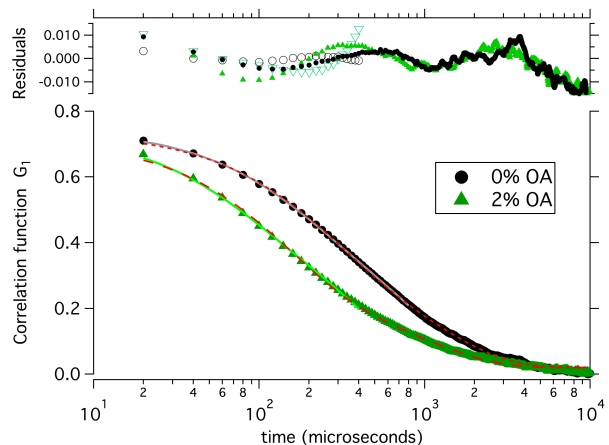


Fig. 4 Correlation function $G_1(t)$ as a function of the correlation time, obtained experimentally by DLS at $T = 20^\circ\text{C}$ for the ferrofluid without added surfactant (full dots) and that with 2 vol% of added OA (full triangles). The lines are the fits done with a development in moments around the mean (Eq. 22 of the work of Frisken in [69]), the residuals are plotted with open symbols. The dashed lines are the fits with two exponentials and the residuals are plotted with the full symbols.

Taking in account that the geometric NP diameter d_{geo} is larger than the magnetic NP diameter $d_m = 9.6$ nm due to a non-magnetic layer of thickness ~ 0.5 nm, associated to the chemisorption bonds of OA chains [49, 68] and considering that the hydrodynamic diameter should be increased by the oleic acid layer, expected to be ~ 1.4 nm [48]. We evaluate the NP's hydrodynamic diameter d_h to 13.4 nm, which is fully consistent with the mean determination of inset of Fig. 3, the mean experimental value of d_h obtained at room temperature at 0 vol% of added OA in Table 2 being slightly too large.

Dynamic Light scattering (DLS)

The collective translation diffusion of the NPs is further probed at 20°C by DLS. Figure 4 shows the field auto-correlation function $G_1(t)$ at room temperature as a function of the correlation time for the two samples at 0 vol% of OA and 2 vol% of OA.

The relaxation $G_1(t)$ is here analyzed in two different ways. Firstly, it is adjusted with a development in terms of moment about the mean, close to the principle of the cumulants, however correcting their weaknesses [69]. Only values in the range $G_1(t) > 0.2$ can be taken into account, which means that the assumed monomodal distribution is not sufficient to describe the system. Secondly, the data are adjusted with two exponentials on the whole range of times. The fits are plotted in Fig. 4 as well as the residuals. The values of D_m and d_h , obtained using Eq. 6 in Sect. 4.2 using the viscosity of pure solvent, are given in Table 2.

Table 2 Diffusion coefficient D_m and hydrodynamic diameter d_h of the particles measured by relaxation of forced Rayleigh scattering (FRS) - averaging 6 measurements as those presented in Fig.2 - and by dynamic light scattering (DLS) at room temperature in ferrofluid samples, with $c = 0$ vol% and 2 vol% of added OA. FRS measurements are analyzed with a single exponential relaxation down to $I_\Phi = 0$ (see Fig. 2). DLS measurements are analyzed in two different ways (i) a development in moments around the mean (columns 4 to 6) - PdI is the polydispersity index, (ii) two exponentials (columns 7 to 11); A is the weight of each exponential. The subscript "long" corresponds to the long experimental relaxation times associated to the largest NPs (see text and Fig. 4).

	FRS (22°C)		DLS _(i) (20°C)			DLS _(ii) (20°C)				
c (vol%)	D_m (m ² /s)	d_h (nm)	D_m (m ² /s)	d_h (nm)	PdI	D_m (m ² /s)	d_h (nm)	D_m^{long} (m ² /s)	d_h^{long} (nm)	A/A^{long}
0.0	$11 \pm 2 \cdot 10^{-12}$	17 ± 3	$4.4 \cdot 10^{-12}$	42	0.59	$6.2 \cdot 10^{-12}$	30	$1.34 \cdot 10^{-12}$	139	1
2.0	$13 \pm 2 \cdot 10^{-12}$	14 ± 3	$9.8 \cdot 10^{-12}$	19	0.65	$11.2 \cdot 10^{-12}$	16.5	$1.6 \cdot 10^{-12}$	119	1.9

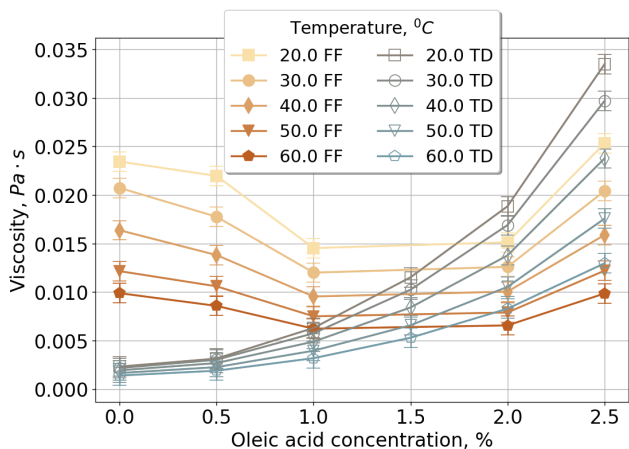


Fig. 5 Viscosity of the ferrofluid η_{FF} (here denoted as FF) and of the fluid-carrier η_{TD} (here denoted as TD) as a function of the concentration of added-surfactant at various temperatures between 20°C and 60°C.

In both fluids, there are small objects (16-30 nm) and much larger ones, the proportion of which decreases when adding oleic acid, as evidenced by A/A^{long} . These large objects are not clearly evidenced by FRS. Indeed these two techniques do not probe the system in the same way. DLS performs, without perturbing the NP organization, an average on the NP's size distribution which is associated to a very high moment of the distribution (of the order of $\langle d^6 \rangle$). It renders DLS particularly sensitive to the presence of some clusters/ aggregates of NPs, more sensitive than the relaxation of FRS [35].

5.3 Viscosimetry

Measurements are performed to establish the relation between shear rate and shear stress. The results, shown at room temperature in Fig. 1-SI of E.S.I., confirm that our ferrofluids display at 20°C a behavior

characteristic of a Newtonian fluid at all relevant surfactant concentration values from $c = 0$ vol% up to 2.5 vol%.

Viscosity is measured at various temperatures, between 20°C and 60°C, both in the ferrofluid and in tetradecane, with various amounts of added surfactant. Fig. 2-SI of E.S.I. presents the T -dependence of the ferrofluid viscosity with the various amounts of added surfactant. As expected the viscosity decreases exponentially as T increases. These variations are analyzed together with those of tetradecane in terms of activation energy E_a in Table 1-SI of E.S.I.. They will be discussed ahead in Sect. 6.

The results at various T , as a function of the concentration of the added amount of surfactant, are summarized in Fig. 5 for the two series of measurements. The measured viscosity of tetradecane at 20°C is $2.31 \pm 0.06 \cdot 10^{-3}$ Pa.s.

From measurements performed at $T = 20^\circ\text{C}$, we see that the viscosity of the ferrofluid with 0% of added OA, is much higher than that of the carrier fluid at the corresponding temperature. It exceeds tetradecane viscosity almost by a factor of ten, showing that Eq. 7 could not apply in this case and that Eq. 8 is more appropriate. It should be noted that such an increase is in any case unusual for this class of surfactant stabilized colloids. We can refer to other papers dealing with tetradecane based ferrofluids stabilized by oleic acid, where values of $\eta_{FF} = 6 \cdot 10^{-3}$ Pa.s [70] and $\eta_{FF} = 7 \cdot 10^{-3}$ Pa.s [71] were given. An increase by an order of magnitude of colloid viscosity relative to that of carrier fluid has been observed at $\Phi = 1.5\%$ in electrostatically aqueous ferrofluids based on hydroxyl-coated NPs with an identified structure of "Sols of clusters" [72]. There, when pH was increased from 2 to 3.5, the NP's surface charge decreased, producing a progressive agglomeration of the NPs and an associated increase by a factor of ten to the

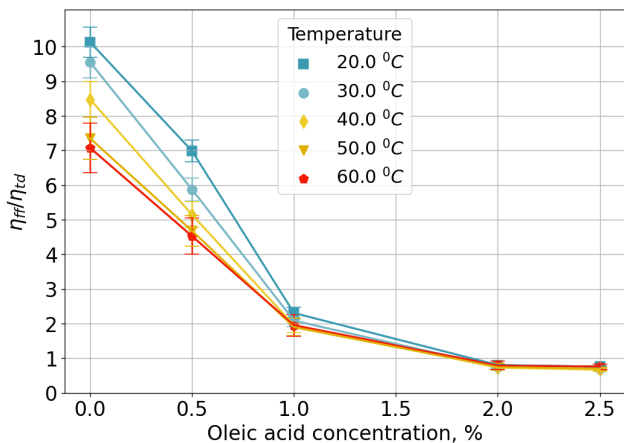


Fig. 6 Ratio of ferrofluid viscosity η_{FF} over η_{TD} , the carrier fluid viscosity with the same added surfactant concentration as a function of surfactant concentration c at various temperatures between $20^{\circ}C$ and $60^{\circ}C$.

relative viscosity of the dispersion.⁷ Unlike in reviewed literature, gel behavior is not apparent in our system. An experimental confirmation of a potential analogy here could be obtained in future research.

We can also observe a marked difference in the characteristics of the two types of fluids (ferrofluid (index FF) and tetradecane without any additives (index TD)). As expected, the viscosity of tetradecane, with added oleic acid, increases as the oleic acid concentration increases. The ferrofluid viscosity follows a more curious trend, slightly decreasing at low added oleic acid concentrations before increasing again, it then reaches values similar to that of the ferrofluid at low percents of added oleic acid and slightly below those of tetradecane with the same percents of added oleic acid.

Similarities of behavior between tetradecane and ferrofluid at high oleic acid concentration values suggest that the very strange pattern of ferrofluid viscosity as a function of vol% of added OA is the result of two antagonistic processes balancing each other at a crossover point, which seems rather independent of temperature.

One of these mechanisms, seen at high oleic acid concentrations, would be just the expected increase of ferrofluid viscosity as free surfactant is added, as it is observed in the carrier fluid. However, the point to elucidate, is why the ferrofluid viscosity is then smaller than that of the solvent with the same quantity of added OA.

⁷This is clear in Fig. 12 of [72]. Under low applied field and large Mason number, the relative viscosity of the dispersions at $\Phi = 1.5\%$ increases by a factor 10 for pH increasing from 2 to 3.5. It is stated in this text that in these conditions the system behavior is close to the zero-field one and in this range of pHs a Sol of clusters is observed.

The second process more enigmatic produces a decrease of viscosity at lower concentrations of added OA.

In an attempt to de-correlate the two effects, Fig. 6 presents the ratio of the ferrofluid viscosity η_{FF} over η_{TD} , the tetradecane viscosity with the same amount of added surfactant. At 0 vol% of added OA, this quantity is the relative viscosity η_r of the ferrofluid, as given by Eq. 8, if the amount of free OA is negligible in the synthesis conditions. At larger percents of added OA, the ratio η_{FF}/η_{TD} would represent the relative viscosity of the ferrofluid, with respect to the fluid carrier (tetradecane + free added chains of OA), if the number of free OA chains is really the number of added OA chains.

The trends are now clear. At high concentration of added surfactant ($c \geq 2$ vol%), temperature and amount of added surfactant do not influence anymore the ratio η_{FF}/η_{TD} . However the calculated ratio η_{FF}/η_{TD} is $\sim 20\%$ smaller than 1 for $c \geq 2$ vol% of added OA, showing that the concentration of free OA in the ferrofluid is slightly smaller than c the added quantity of OA for $c \geq 2$ vol% of added OA.

Let us now analyze and discuss these results in the two conditions of FRS and DLS measurements, namely at $c = 0$ and 2 vol% of added OA.

5.3.1 Analysis at 0 vol% of added OA

Let us first analyze the ratio η_{FF}/η_{TD} at 0 vol% of added OA with Eq. 8, assuming a structure of Sols of clusters as described in [73], [72] and deducing Φ_h as a function of T . From this large hydrodynamic volume fraction, we can calculate a mean hydrodynamic radius of the dispersed objects by making several hypothesis on the shape of these objects. For example (i) assuming that the NPs are individually dispersed, then [74]:

$$d_h^{(i)} = d_m \left(\frac{\Phi_h}{\Phi_m} \right)^{0.33} \quad (15)$$

or (ii) assuming that two NPs are enclosed in each dispersed object forming dimers of NP, then:

$$d_h^{(ii)} = d_m \left(\frac{2\Phi_h}{\Phi_m} \right)^{0.33} \quad (16)$$

d_m and Φ_m being respectively the magnetic diameter and the magnetic volume fraction of individual NPs in solution, which are known and given in Sect. 3. We obtain $d_h^{(i)} = 22.3 \pm 0.01$ nm and $d_h^{(ii)} = 28.1 \pm 0.01$ nm at $T = 20^{\circ}C$. They remain almost constant with T as they decrease down to $d_h^{(i)} = 22.1 \pm 0.01$ nm and $d_h^{(ii)} = 27.9 \pm 0.01$ nm at $T = 60^{\circ}C$. In fact, the observed T -dependence of η_{FF}/η_{TD} , is not connected with a large

T -dependence of the hydrodynamic diameter of the dispersed objects. Obviously, $d_h^{(i)} = 22.3$ nm is too large to be associated with a monolayer coating of magnetic NPs [52], and the hypothesis (ii) of dispersed dimers with

$$d_h^{(ii)} \sim 28 \text{ nm}$$

seems more reasonable. The more so that

$$d_h^{(ii)}/2 \sim 14 \text{ nm}$$

is quite close to the evaluation of 13.4 nm obtained for the hydrodynamic diameter of NPs coated with a monolayer of OA given in Sect. 4.1. Moreover $d_h^{(ii)} = 28.1$ nm is also quite close to the DLS short-time d_h value obtained here at room temperature with 0 vol% of added OA (see Table 2)⁸.

Thus, under this interpretation at 0 vol% of added OA, viscosity measurements evidence the presence of dimers/small clusters of NPs in the dispersion. They are globally coated by a monolayer of surfactant, inside which the OA density per NP is smaller than the saturated value for individual NPs.

5.3.2 Analysis at 2 vol% of added OA

At room temperature and 2 vol% of added OA, both DLS and FRS roughly converge (at short times) towards comparable hydrodynamic diameters of the order of 15 nm (also close to the values given just above for individual NPs). Using Eq. 8 and Eq. 15, with $d_h^{(i)} = 15$ nm, we can calculate Φ_h and the reduced viscosity η_r where η_{FF} is normalized by the viscosity of the fluid carrier (tetradecane + free OA). As at 2 vol% of added OA, η_{FF} is determined, we can deduce the viscosity of the fluid carrier; At $T = 20^\circ\text{C}$, it equals $\sim \eta_{FF}/1.09 \sim 0.0139$ Pa.s At this temperature, the viscosity of tetradecane with 2 vol% of added OA equals 0.0188 Pa.s. By interpolation of the measurements of the viscosity of tetradecane with added OA from Fig. 5, we obtain ~ 0.0139 Pa.s at ~ 1.7 vol% of free OA in tetradecane, meaning that at 2 vol% of added OA in the ferrofluid, the NP's coating is increased by roughly 0.3 vol% of OA, which adsorbs on the NPs while only ~ 1.7 vol% remains in solution. Note that roughly the same evaluation of ~ 0.3 vol% of OA adsorbed on the NPs is obtained for 2.5 vol% of added OA, at $T = 20^\circ\text{C}$ with the same hypothesis of $d_h \sim 15$ nm. At $T = 60^\circ\text{C}$, proceeding in the same way we obtain a slightly larger quantity ~ 0.4 vol% of adsorbed OA.

⁸An analysis in terms of clusters of 3 (resp. 4) NPs would lead to a mean hydrodynamic diameter of clusters of 32.2 nm (resp. 35.4 nm), which are slightly larger (but almost compatible) with the short-time DLS determination.

5.3.3 Evaluation of the NP coating and of the free OA concentration in the synthesis conditions

So, the potential explanation for the initial decrease of ferrofluid viscosity would involve an initial surfactant layer around the NPs which is not complete (explaining the existence of dimers and possible clusters at 0 vol% of added OA) and a progressive saturation of this surfactant layer as OA is added, destroying progressively the dimers and some of the clusters seen in DLS.

A tentative evaluation of this incomplete saturation in the initial conditions at 0% of added OA can be obtained by using the work of Ref. [55] with maghemite NPs dispersed in cyclohexane, thanks to an oleic acid coating. In [55], the saturation of the OA layer on the NPs corresponds to ~ 3.5 OA molecules per nm^2 . It means here for NPs of typical diameter 10 nm at a magnetic volume fraction of $\sim 5\%$, a total quantity of OA of the order of 0.17 mol/L. Adding 0.3 vol% of OA to the NP coating, represents roughly 10^{-2} mol/L of added OA in solution and $\sim 6\%$ ($=1/17$) of the saturation coating. This could give an evaluation of the initial incomplete coating in the synthesis conditions, of the order of ~ 3.3 OA molecules per nm^2 . According to Fig. 1 of [55], it is already very close to the saturation plateau. It could explain the good colloidal stability of the initial system, allowing anyway the formation of NP's dimers (or clusters).

Moreover, still using Fig. 1 of [55], it is also possible to evaluate the concentration of free OA in the initial conditions. A coating of ~ 3.3 OA molecules per nm^2 corresponds to a concentration of free OA of $\sim 5 \cdot 10^{-3}$ mol/L, that is roughly ~ 0.15 vol% of free OA, which is rather low and compatible with the observations of [48].

6 Discussion

So from the analysis of viscosity measurements we propose an interpretation, according to which:

(i) At 2 vol% of added surfactant, the mono-layer of surfactant on the NP's surface is saturated at ~ 3.5 OA per nm^2 in tetradecane with a concentration of free OA ~ 1.7 vol%. In that situation, NPs are mostly individually dispersed.

(ii) At 0 vol% of added surfactant, the mono-layer of surfactant on the NP's surface is not completely saturated at ~ 3.2 OA per nm^2 in tetradecane with a concentration of free OA ~ 0.15 vol%. In that situation, the ferrofluid is stable from a colloidal point of view but the NPs are slightly clustered, mostly as dimers.

These observations are compatible with DLS measurements at room temperature, however a question is

remaining. Why these dimers/ small clusters at 0 vol% of added surfactant evidenced by DLS and viscosity are not clearly observed in FRS relaxation, even if FRS detects a few aggregates?

A proposition could be that the FRS gradient of temperature (even if small) is able to produce at the surface of the present NPs, coated with surfactant by chemisorption, a tangential stress [38] which could induce lateral migration of some surfactant chains in the non-saturated monolayer along the surface (as for liquid drops [67]). It would produce a surface reorganization of surfactant with surface gradients that can locally break the dimer's links in the gradient of T . Such breakings of aggregates are never observed in water with NPs stabilized with surfactant chains as then a bilayer is evolved [52]. It is also not observed with NPs electrostatically stabilized because the surface charge of the solid particle is usually homogeneous, but it could happen here because of the non-saturation of the monolayer at 0 vol% of added surfactant.

Let us analyze now the Soret coefficient S_T in terms of NP thermophobicity Q^* , the heat of transport of the NPs in the carrier fluid. We can deduce here Q^* as a function of T and of added c using Eq. 2 and the definition of the NP Eastman entropy of transfer \hat{S}_{NP} with the following expression:

$$Q^* = T\hat{S}_{NP} = TS_T \frac{kT}{\chi} \quad (17)$$

Using the experimental values of S_T and (as previously) the compressibility hard sphere value $\chi = 0.67$, Fig. 7 presents Q^* as a function of T for 0 vol% and 2 vol% of added OA. At 2 vol% of added OA, $Q^* = 2.4 \pm 0.3$ eV without any marked T dependence.

At 0 vol% of added OA, Q^* presents a slightly different behavior as a function of T . However it is difficult to incriminate diffusiophoresis taking in account the very low value of free OA in these conditions. Anyway, due to the unsaturated layer of surfactant on the NPs, the NP-NP interaction parameter χ could be slightly larger at 0 vol% of OA than at 2 vol% of OA. Slightly increasing χ (more attractive NP-NP interaction) would slightly decrease \hat{S}_{NP} and Q^* . A value $\chi = 0.80$ (instead of 0.67) at 0 vol% of OA would bring its Q^* at the same mean value $\langle Q^* \rangle = 2.4$ eV as that at 2 vol% of added OA with $\chi = 0.67$ (see Fig. S2 of E.S.I.). Note that, as it is shown in Sect. S2 of E.S.I., this increase of χ does not modify here the various d_h determinations.

The last point to discuss is the activation energy E_a deduced from thermal variations of viscosity measurements, presented in Sect. 1 of E.S.I. Fig. 8 shows the activation energy as a function of the concentration c of

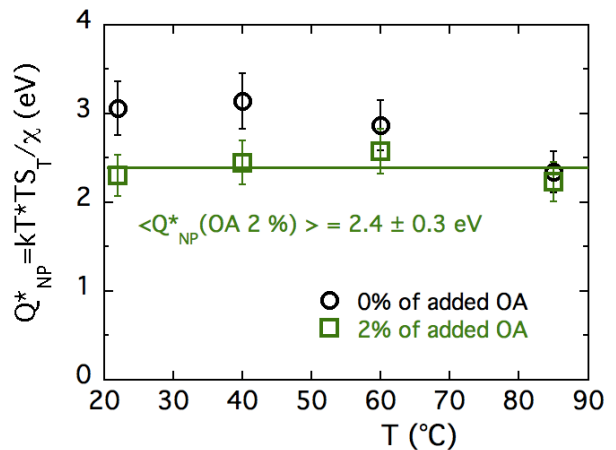


Fig. 7 Enthalpy of transport Q^* of the NPs deduced from the FRS measurements as a function of T for the two probed surfactant concentrations c .

added surfactant, both for the tetradecane and for the ferrofluid. Tetradecane with added surfactant presents a linear variation as a function of c from $E_a(\text{TD}) = 0.14$ eV for pure tetradecane at 0 added surfactant with a slope corresponding to 0.049 eV per 1 vol% of free OA in tetradecane (or equivalently $E_a(\text{free OA}) - E_a(\text{TD})$ equals 1.52 eV per mol/L of free OA in tetradecane).

For its part, the activation energy of the ferrofluid, is at the first order independent of c with $E_a(\text{FF}) \sim 0.19$ eV, even if distortions are present, in particular at 0 vol% of added OA, clearly outside the error bar, distortions which could be associated to the orientation/deformation of the clusters. More or less $E_a(\text{FF})$ equals the activation energy of tetradecane with 1 vol% of free OA. However no direct conclusion can be taken as activation energy contains both an enthalpic contribution and an entropic one $E_a = \Delta H - T\Delta S$, as shown in [75], the liquid carrier and the NP's dispersion may present almost the same E_a value with a different distribution among enthalpy and entropy. Precise density measurements would be necessary to really conclude on these points for the ferrofluid (see [75]).

However let us try, using the determined values of $E_a(\text{TD} + \text{free OA})$, to evaluate the activation E_a per NP associated to the surfactant chains of the saturated monolayer in tetradecane, in order to compare it to the heat of transport Q^* per NP at 2 vol% of added OA.

With a geometrical NP diameter $d_{\text{geo}} = 10.6$ nm, the number of OA chains in the surfactant monolayer is $3.6\pi d_{\text{geo}}^2 = 1270$ per NP. In terms of number of moles per liter in the surfactant layer (of volume $\pi(d_h^3 - d_{\text{geo}}^3)/6 = 1176$ nm³ with $d_h = 15$ nm), it gives $n = 1.85$ mol/L of bounded OA in the surfactant layer of one NP. Mean-

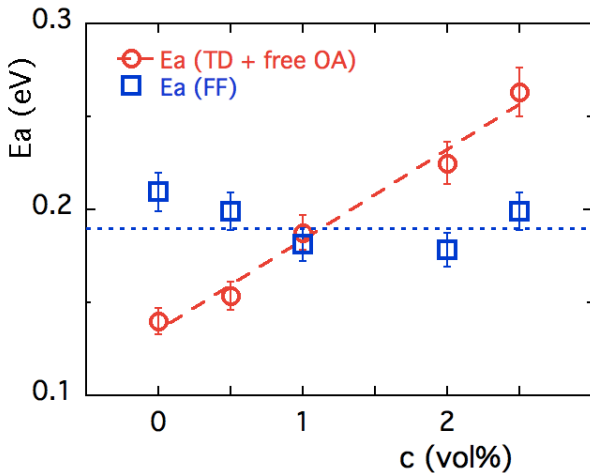


Fig. 8 Activation energy E_a deduced from the viscosity measurements of the ferrofluid ($E_a(\text{FF})$) and of the tetradecane ($E_a(\text{TD} + \text{free OA})$) as a function of the concentration c of added OA. The dashed line is the best linear fit of $E_a(\text{TD} + \text{free OA})$ as a function of c (see the text for numbers). The dotted line corresponds to the mean value of $E_a(\text{FF}) \sim 0.19$ eV.

ing that in the surfactant layer there is ~ 58 vol% of OA and ~ 42 vol% of TD.

Using for the activation energy $E_a(\text{free OA}) - E_a(\text{TD}) = 1.52$ eV per mol/L of free OA in tetradecane (extrapolated at higher c and forgetting the loss of entropy for the bounded OA chains), we obtain an activation energy, associated to the bounded OA, of ~ 3 eV per NP. An evaluated value of the same order of magnitude as the heat of transport per NP $Q^* = 2.4 \pm 0.3$ eV per NP obtained from FRS measurements in Fig. 7, the difference being ascribed to the neglected loss of entropy of the surfactant chains, which is difficult to quantify.

7 Conclusion

A series of ferrofluids based on magnetite particles, dispersed in tetradecane and stabilized with a surfactant-coating of oleic acid (OA) are probed here by Forced Rayleigh scattering (FRS) for various added concentrations c of oleic acid. OA which is fully miscible in tetradecane, forms a monolayer at the surface of the NPs.

The Soret coefficient S_T and the mass diffusion coefficient D_m of the nanoparticles are measured by FRS as a function of temperature T for various added c of oleic acid, in excess with respect to the initial sample. These results are compared to DLS and macroscopic rheological measurements.

For the two probed concentrations of added oleic acid (0 and 2 vol%), the measured Soret coefficient is

found positive whatever T , expressing the thermophobicity of the NPs. The obtained values of S_T are however much larger than in the former measurements in porous media. This allows to conclude that the significant decrease and inversion of sign of S_T following the addition of excess surfactant that has been previously reported for ferrofluid in a porous environment is in large part a result of interaction with the porous environment itself.

In the sample with no added surfactant, viscosity measurements appear to indicate the presence of dimers or small clusters. These clusters tend to disappear with added OA concentrations $c \geq 2$ vol%. Both observations are backed by DLS measurements at room temperature. By opposition, FRS relaxation, which is less sensitive to the presence of clusters than DLS and viscosity, evidences mainly individually dispersed NPs. A tentative explanation could be a non-saturated monolayer of surfactant in the initial conditions (0 vol% of added OA) favoring small NP's clusters in non-perturbed situations; The presence of small temperature gradients in the FRS experiment being able to induce gradients of surfactant in the NPs' surface layer partially destroying the labile clusters.

It should be emphasized that this is an interpretation of our experimental data and direct measurements regarding several aspects are lacking, such as those concerning surfactant distribution within the colloid, direct structural probing of the cluster formation at 0% of added OA as in [73], and cluster dissolution when adding OA. As such, the high values of viscosity at low oleic acid concentrations and the subsequent reduction of those values cannot be said to be here well understood at this stage of research.

By comparison with literature measurements, we deduce from the viscosity determinations at 0 vol% (resp. 2 vol%) of added OA, an evaluation of the density of coating ~ 3.2 (resp. ~ 3.5) OA per nm^2 and of the value of free OA concentration ~ 0.15 % (resp. ~ 1.7 %). Moreover from the temperature variations of tetradecane viscosity with free added OA, it is possible to evaluate the activation energy of the surfactant chains in the (saturated) monolayer around the NPs. It is found of the same order of magnitude as the heat (enthalpy) of transport Q^* of the NP (marking their thermophobicity) deduced from the Soret coefficient determinations. $Q^* = 2.4 \pm 0.3$ eV per NP is found independent of T for the NPs with a saturated surfactant layer at 2 vol% of added OA and behaving as hard spheres. This same value of Q^* is obtained at 0 vol% of added OA, providing the hypothesis that the interparticle interaction is then slightly less repulsive than hard spheres - an hypothesis quite reasonable taking in ac-

count the observation of clusters by DLS and viscosity in these conditions.

To go further, in particular to check if diffusiophoresis of free surfactant is involved in the thermophoretic process, precise determinations of the concentration of free species and of their thermophoretic behavior would be mandatory. Moreover measurements at different NP volume fractions and different temperatures would be necessary, in association with a SANS probing of the interaction, to determine directly how the compressibility of the NP system evolves with the coating density towards the hard sphere situation when the coating is fully saturated.

8 Acknowledgments

We thank Ansis Mezulis for consultations on experimental work, Guillaume Mériquet and Mikhail S. Krakov for useful discussions and Amandine Anfry, Michail M. Maiorov and Frédéric Gélébart for technical support in the experiments.

Author contribution statement

Viesturs Sints: Conceptualization, Investigation, Writing - Original Draft

Mitradeep Sarkar: Methodology, Investigation

Jesse Riedl: Methodology

Gilles Demouchy: Methodology, Investigation

Emmanuelle Dubois: Methodology, Investigation

Régine Perzynski: Conceptualization, Writing - Original Draft, Supervision

Dmitry Zablotsky: Investigation

Gunars Kronkalns: Methodology, Resources

Elmars Blums: Conceptualization, Supervision

Funding

Latvian State Research Program IMIS2 PHC OSMOSE 2018 contract n°40033S between France and Latvia

Declarations of interest: none

References

1. E. Shojaeizadeh, F. Veysi, K. Goudarzi, *Applied Thermal Engineering* **164**, 114510 (2020). DOI 10.1016/j.applthermaleng.2019.114510
2. M. Vasilakaki, I. Chikina, V.B. Shikin, N. Ntallis, D. Peddis, A.A. Varlamov, K.N. Trohidou, *Applied Materials Today* **19**, 100587 (2020). DOI 10.1016/j.apmt.2020.100587
3. J.H. Kim, H.S. Seo, Y.J. Kim, *Micromachines* **9**(9), 457 (2018). DOI 10.3390/mi9090457
4. Q. Jiang, B. Rogez, J.B. Claude, G. Baffou, J. Wenger, *Nano Letters* **12**, 8811 (2020). DOI 10.1021/acs.nanolett.0c03638
5. D. Zablotsky, M.M. Maiorov, *Int. J. Heat Mass Transfer* **164**, 120552 1 (2021). DOI 10.1016/j.ijheatmasstransfer.2020.120552
6. D. Zablotsky, A. Mezulis, E. Blums, M. Maiorov, *Phil. Trans. R. Soc. A* **380**, 20200310 1 (2022). DOI 10.1098/rsta.2020.0310
7. G. Mériquet, G. Demouchy, E. Dubois, R. Perzynski, A. Bourdon, *J. Non-Equilib. Thermodyn.* **32**, 271 (2007). DOI 10.1515/JNETDY.2007.019
8. A.L. Sehnem, A.M.F. Neto, D. Niether, S. Wiegand, *Phys. Rev. E* **98**, 062615 (2018). DOI 10.1103/PhysRevE.98.062615
9. R. Cabreira-Gomes, A. Ferreira da Silva, M. Kouyaté, G. Demouchy, G. Mériquet, R. Aquino, E. Dubois, S. Nakamae, M. Roger, J. Depeyrot, R. Perzynski, *Phys. Chem. Chem. Phys.* **20**, 16402 (2018). DOI 10.1039/c8cp02558d
10. M. Kouyaté, C. Filomeno, G. Demouchy, G. Mériquet, S. Nakamae, V. Peyre, M. Roger, A. Cebers, J. Depeyrot, E.D. and R. Perzynski, *Phys. Chem. Chem. Phys.* **21**, 1895 (2019). DOI 10.1039/c8cp06858e
11. M. Sarkar, J.C. Riedl, G. Demouchy, F. Gélébart, G. Mériquet, V. Peyre, E. Dubois, R. Perzynski, *Eur Phys J E Soft Matter* **42**(6), 72 1 (2019). DOI 10.1140/epje/i2019-11835-6
12. R.Y. Dong, Y. Zhou, C. Yang, B.Y. Cao, *Journal of Physics: Condensed Matter* **27**, 495102 (2015). DOI 10.1088/0953-8984/27/49/495102
13. O. Syshchyk, D. Afanasenkau, Z. Wang, H. Kriegs, J. Buitenhuis, S. Wiegand, *Eur. Phys. J. E* **39**, 129 (2016). DOI 10.1140/epje/i2016-16129-y
14. H. Ning, J. Buitenhuis, J. Dhont, S. Wiegand, *J. Chem. Phys.* **125**, 204911 1 (2006). DOI 10.1063/1.2400860
15. E. Blums, G. Kronkalns, M.M. Maiorov, A. Mezulis, *J. Magn. Magn. Mat.* **289**, 275 (2005). DOI 10.1016/j.jmmm.2004.11.078
16. V. Sints, E. Blums, M. Maiorov, G. Kronkalns, *Eur Phys J E Soft Matter* **38**(5), 119 (2015). DOI 10.1140/epje/i2015-15035-2
17. V. Sints, E. Blums, G. Kronkalns, K. Erglis, M. Maiorov, *Int. J. Heat Mass Transfer* **125**, 580 (2018). DOI 10.1016/j.ijheatmasstransfer.2018.04.078
18. V. Yasnou, A. Mialdun, D. Melnikov, V. Shevtsova, *International Journal of Heat and Mass Transfer* **143**, 118480 (2019). DOI 10.1016/j.ijheatmasstransfer.2019.118480
19. S.D. Lecce, T. Albrecht, F. Bresme, *Nanoscale* **12**, 23626 (2020). DOI 10.1039/D0NR04912C
20. A. Würger, *Comptes Rendus Mécanique* **341**(4), 438 (2013). DOI 10.1016/j.crme.2013.02.006. 10th International Meeting on Thermodiffusion
21. R. Piazza, A. Parola, *Journal of Physics: Condensed Matter* **20**(15), 153102 (2008). DOI 10.1088/0953-8984/20/15/153102
22. B.V. Derjaguin, G.P. Sidorenkov, *Dokl. Acad. Nauk SSSR* **32**, 622 (1941)
23. E. Ruckenstein, *J. Colloid Int. Sci.* **83**, 77 (1981). DOI 10.1016/0021-9797(81)90011-4
24. J.L. Anderson, *Ann. Rev. Fluid Mech.* **21**, 61 (1989). DOI 10.1146/annurev.fl.21.010189.000425
25. K.I. Morozov, in *Thermal Nonequilibrium Phenomena in Fluid Mixtures, Lecture Notes in Physics*, vol. 584, ed. by W. Köhler, S. Wiegand (Springer-Verlag, 2002), *Lecture Notes in Physics*, vol. 584, p. 38
26. G. Demouchy, A. Mezulis, A. Bee, D. Talbot, J. Bacri, A. Bourdon, *J. Phys. D: Appl. Phys.* **37**, 1417 (2004). DOI 10.1088/0022-3727/37/10/002

27. T. Salez, S. Nakamae, R. Perzynski, G. Mériquet, A. Cebers, M. Roger, *Entropy* **20**, 405 1 (2018). DOI 10.3390/e20060405
28. A. Parola, R. Piazza, *Eur Phys J E Soft Matter* **15**(3), 255 (2004). DOI 10.1140/epje/i2004-10065-5
29. S. Iacopini, R. Piazza, *Europhys. Lett.* **63**, 247 (2003). DOI 10.1209/epl/i2003-00520-y
30. S. Iacopini, R. Rusconi, R. Piazza, *Eur Phys J E Soft Matter* **19**, 59 (2006). DOI 10.1140/epje/e2006-00012-9
31. R.G. Larson, *The Structure and Rheology of Complex Fluids* (Oxford University Press, Oxford, New York, 1998)
32. B. Berkovsky (ed.), *Magnetic Fluids and Applications Magnetic Fluids and Applications Handbook* (Begell House Inc. Publ., 1996)
33. M. Abareschi, S.H. Sajjadi, S.M. Zebarjad, E.K. Goharshadi, *Journal of Molecular Liquids* **163**(1), 27 (2011). DOI 10.1016/j.molliq.2011.07.007
34. J. Tothova, J. Kovac, P. Kopcansky, M. Rajnak, K. Paulovicova, M. Timko, A. Jozefczak, *Acta Physica Polonica A* **126**(1), 278 (2014). DOI 10.12693/APhysPolA.126.278
35. P. Rossmannith, W. Kohler, *Macromolecules* **29**, 3203 (1996). DOI 10.1021/ma9516302
36. J.N. Agar, C.Y. Mou, J.L. Lin, *J. Phys. Chem.* **93**, 2079 (1989). DOI 10.1021/j100342a073
37. A. Wurger, *Phys. Rev. Lett.* **101**, 108302 1 (2008). DOI 10.1103/PhysRevLett.101.108302
38. W. Kohler, K. Morozov, *J. Non-Equilib. Thermodyn.* **41**(3), 151 (2016). DOI 10.1515/jnet-2016-0024
39. G. Wittko, W. Kohler, *Europhys. Lett.* **78**, 46007 (2007). DOI 10.1209/0295-5075/78/46007
40. S. Mohanakumar, J. Luettmer-Strathmann, S. Wiegand, *J. Chem. Phys.* **154**, 084506 (2021). DOI 10.1063/5.0038039
41. J.K.G. Dhont, S. Wiegand, S. Duhr, D. Braun, *Langmuir* **23**(4), 1674 (2007). DOI 10.1021/la062184m
42. G.D.J. Phillies, *J. Chem. Phys.* **60**(3), 976 (1974). DOI 10.1063/1.1681177
43. N.F. Carnahan, K.E. Starling, *J. Chem. Phys.* **53**(2), 600 (1970). DOI 10.1063/1.1674033
44. G.K. Batchelor, *J. Fluid Mech.* **119**, 379 (1982). DOI 10.1017/S0022112082001402
45. D.M. Heyes, H. Sigurgeirsson, *J. of Rheology* **48**, 223 (2004). DOI 10.1122/1.1634986
46. C. Berli, D. Quemada, *Langmuir* **16**, 7968 (2000). DOI 10.1021/la000365x
47. G. Kronkalns, M. Kodols, M.M. Maiorov, *Latv. J. Phys. Tech. Sci.* **50**(4), 56 (2013). DOI 10.2478/lpts-2013-0026
48. M. Avdeev, D. Bica, L. Vékás, V. Aksenov, A. Feoktystov, O. Marinica, L. Rosta, V. Garamus, R. Willumeit, *J. Colloid Int. Sci.* **334**, 37 (2009). DOI 10.1016/j.jcis.2009.03.005
49. M.M. Maiorov, D. Zablotzky, E. Blums, A. Krumina, *IOP Conf. Ser.* **503**, 012029 (2019). DOI 10.1088/1757-899X/503/1/012029
50. T.V. Santos, M.F. Pereira, H.M. Avelino, F.J. Caetano, J.M. Fareleira, *Fluid Phase Equilibria* **453**, 46 (2017). DOI 10.1016/j.fluid.2017.08.025
51. S. Rath, N. Sinha, H. Sahoo, B.Das, B.K.Mishra, *Applied Surface Science* **295**, 115 (2014). DOI 10.1016/j.apsusc.2014.01.014
52. A. Hoell, M. Kammel, A. Heinemann, A. Wiedenmann, *J. Appl. Cryst.* **36**, 558 (2003). DOI 10.1107/S0021889803001742
53. D. Susan-Resiga, V. Socoliuc, T. Boros, T. Borbáth, O. Marinica, A. Han, L. Vékás, *Journal of Colloid and Interface Science* **373**(1), 110 (2012). DOI 10.1016/j.jcis.2011.10.060
54. C. Tanford, *J. Phys. Chem.* **76**, 3020 (1972). DOI 10.1021/j100665a018
55. E. Dubois, V. Cabuil, F. Boué, R. Perzynski, *J. Chem. Phys.* **111**(15), 7147 (1999). DOI 10.1063/1.480007
56. H.F. Eicke, in *Micelles* (Springer Berlin Heidelberg, Berlin, Heidelberg, 1980), pp. 85–145
57. A. Khoshnood, A. Firoozabadi, *Langmuir* **31**(22), 5982 (2015). DOI 10.1021/la504658u. PMID: 25941967
58. V. Petrenko, M. Avdeev, V.L. Aksenov, L. Bulavin, L. Rosta, in *Magnetism and Magnetic Materials, Solid State Phenomena*, vol. 152 (Trans Tech Publications Ltd, 2009), *Solid State Phenomena*, vol. 152, pp. 198–201. DOI 10.4028/www.scientific.net/SSP.152-153.198
59. L.A. Bulavin, A.V. Nagorny, V.I. Petrenko, M.V. Avdeev, L. Alm'asy, L. Rosta, V.L. Aksenov, *Ukrainian Journal of Physics* **58**(12), 1143 (2013). DOI 10.15407/ujpe58.12.1143
60. W.R. Klein, C.B. Tipnis, E.A. Hiedemann, *J. Acoust. Soc. Amer.* **38**, 229 (1965). DOI 10.1121/1.1909641
61. W.R. Klein, *Proc. I.E.E.E.* **54**(5), 803 (1966). DOI 10.1109/PROC.1966.4866
62. H. Kogelnik, *Bell Syst. Tech. J.* **48**(9), 2909 (1969). DOI 10.1002/j.1538-7305.1969.tb01198.x
63. C. Wohlfarth, B. Wohlfarth, in *Refractive Indices of Inorganic, Organometallic, and Organononmetallic Liquids, and Binary Liquid Mixtures*, vol. 38A, ed. by M.D. Lechner (Springer-Verlag, 1996), vol. 38A, p. 38. DOI 10.1007/10478514_3
64. J.C. Maxwell Garnett, *Proc. R. Soc. Lond.* **76**(511) (1905). DOI 10.1098/rspa.1905.0039
65. C. Filomeno, M. Kouyaté, V. Peyre, G. Demouchy, A. Campos, R. Perzynski, F. Tourinho, E. Dubois, *J. Phys. Chem. C* **121**, 5539 (2017). DOI 10.1021/acs.jpcc.6b10280
66. T. Fiuza, M. Sarkar, J.C. Riedl, A. Cebers, F. Cousin, G. Demouchy, J. Depeyrot, E. Dubois, F. Gélébart, G. Mériquet, R. Perzynski, V. Peyre, *Soft Matter* **17**, 4566 (2021). DOI 10.1039/d0sm02190c
67. J. Chen, K.J. Stebe, *Journal of Fluid Mechanics* **340**, 35 (1997). DOI 10.1017/S0022112097005156
68. P. Dutta, S. Pal, M.S. Seehra, N. Shah, G.P. Huffman, *Journal of Applied Physics* **105**(7), 07B501 (2009). DOI 10.1063/1.3055272
69. B.J. Frisken, *Applied Optics* **40**(24), 4087 (2001). DOI 10.1364/AO.40.004087
70. M. Hangi, M. Bahiraei, A. Rahbari, *Advanced Powder Technology* **29**(9), 2168 (2018). DOI https://doi.org/10.1016/j.apt.2018.05.026
71. E. Blums, V. Sints, A. Mezulis, G. Kronkalns, *Magnetohydrodynamics* **49**(3-4), 360 (2013)
72. C. Galindo-Gonzalez, A. Ponton, A. Bee, J. Chevalet, D. Talbot, R. Perzynski, E. Dubois, *Rheologica Acta* **55** (2016). DOI 10.1007/s00397-015-0892-5
73. B. Frka-Petesic, E. Dubois, L. Almasy, V. Dupuis, F. Cousin, R. Perzynski, *Magnetohydrodynamics* **49**(3/4), 328 (2013). DOI 10.22364/mhd.49.3-4.15
74. A. Bahandari, *J. Magn. Magn. Mat. to appear* (2022). DOI 10.1016/j.jmmm.2021.168975
75. C. Kern, R. Aquino, E. Dubois, R. Perzynski, V. Peyre, *Journal of Molecular Liquids* **268**, 545 (2018). DOI 10.1016/j.molliq.2018.07.063